euronoise

Observations and modeling of angular compression and vertical spatial coherence in sea surface forward scattering

Peter Dahl

Applied Physics Laboratory, University of Washington, 1013 NE 40th St, Seattle, WA 98105, USA
dahl@apl.washington.edu

Measurements and modeling of spatial coherence and related angular spreading associated with forward scattering from the sea surface are presented. The van Cittert-Zernike theorem is used in the modeling. The measurements were conducted in waters 80 m deep off the North American continental shelf as part of Shallow Water 06 (August 2006). Acoustic signals were recorded on a vertical line array of length 1.4 m centered at depth 25 m. The source (1-20 kHz) was deployed at depth 40 m from the R/V *Knorr*, at range 200 m from the MORAY. Conditions were characterized by a downward-refracting profile, e.g., sound speed going from 1530 m/s at the surface to 1485 m/s at depth 25 m. Refraction modifies the vertical angular spread due to rough sea surface scattering, which can be understood from Snell's law. The Snell mapping is smooth, so a Taylor expansion around the mean grazing angle provides a functional relation between the angular variance near the surface and that at the receiver. The latter is measurably reduced owing to refraction, the effect called angular compression.

1 Introduction

Propagation over short ranges in shallow water, i.e., ranges of the order of a few depths, is strongly influenced by sound interaction with the sea surface. For frequencies of O(10) kHz and above this interaction is often better described by a forward scattering, rather than a reflection process. The direct-, single surface bounce-, and single bottom bounce-paths, can in many environments dominate the intensity impulse response [1]. However it is the sea surface bounce path that undergoes the majority of the time and angle spreading. For example, the vertical spatial coherence of the combination of these three arrivals undergoes oscillation owing to the coherent combination of paths of differing arrival angles, but the magnitude of coherence is strongly influenced by angular spread imparted on the surface bound path.

In this paper, results of an experiment to measure the spatial coherence of sound forward scattered from the sea surface are discussed. The experiment was part of Shallow Water '06 (SW06). The acoustic observations were made by the University of Washington Applied Physics Laboratory (APL-UW) from aboard the research vessel R/V *Knorr*. An acoustic source (1-20 kHz) was deployed at depth 40 m from the stern of the R/V *Knorr*, and signals were recorded on a moored receiving array system (MORAY), with remotely changeable receiving configurations. Results presented here are from the 1.4 m vertical line array centered at depth 25 m composed of 4 omni-directional hydrophones.

The MORAY was placed at position 39.0245 N, 73.0377 W (depth 80 m) for SW06; a location that defined the central site for SW06 experimental observations in the mid-frequency range [2]. The acoustic source-receiver geometry was established by the position (station) of the R/V *Knorr*. Here we focus on the measurements made on August 10 between 0830-1500 UTC, at four stations each at range 200 m from the MORAY and separated in direction between source and receiver by 90°. Station-keeping by the R/V *Knorr* was made precise by its dynamic positioning system, and repeated measurements from these four stations for other measurements over the course of 7 days showed fluctuations in range of less than 5 m.

2 Environmental Conditions

2.1 Sound Speed Conditions

The sound speed conditions were characterized by a downward-refracting sound speed profile (Fig. 1), e.g., sound speed going from 1530 m/s at the surface to 1485 m/s at depth 25 m. This, as we shall demonstrate, is a key environmental driver in determining vertical spatial coherence.

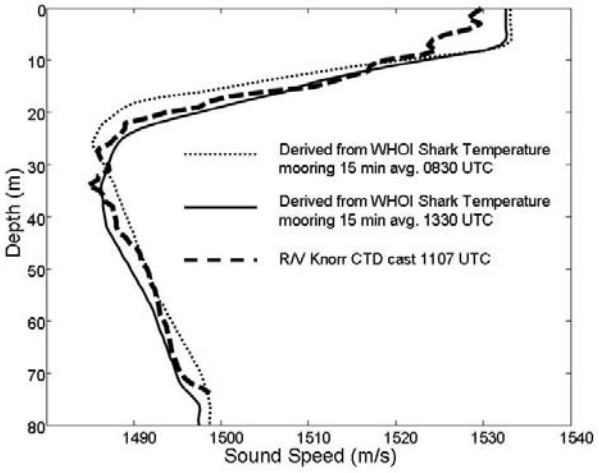

Fig.1 Nominal sound speed conditions for period 0830-1500 UTC 10 August 2006 as measured by a Conductivity –Depth-Temperature (CTD) profiler deployed from the R/V *Knorr*, and inferred from a nearby WHOI temperature mooring.

2.2 Wind and Wave Conditions

Sea surface directional wave measurements were made using a 0.9-m diameter TRIAXYS directional wave buoy deployed by APL-UW 800 m from the MORAY site, and also by the Air-Sea Interaction Spar (ASIS) buoy deployed by the University of Miami 1.5 km from the MORAY site. An interesting comparison of the two measures is shown in Fig. 2 (b), representing an average of each of the two measurement systems between 0830 and 1500 UTC on August 10th, expressed in terms of a directional averaged wave spectrum. The rms wave height H is 0.16 m, although slightly less for the ASIS (0.14 m). Apart from this difference, both systems recorded relatively unchanging spectra during this period, with rms wave height differing

by no more than +/- 10% over the long-term average between 0830 and 1500. For subsequent acoustic modelling the long-term average spectrum from ASIS will be used, as its temporal resolution is higher (1 Hz). Figure 1 (a) is a display of the averaged directional wave properties from the TRIAXYS buoy, showing a swell system originating from the south and a wave-wind system originating from the southwest. The ASIS also recorded wind speed with 6 m/s (+/- 1 m/s) representative of the entire 6.5 h measurement period.

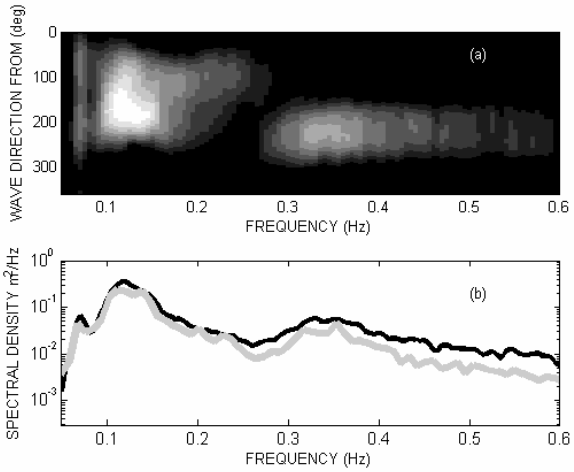

.Fig.2 (a) Average directional wave spectrum for period 0830-1500 UTC 10 August 2006 as measured 800 m from MORAY. (b) Average non-directional wave spectrum as measured 800 m from MORAY, with TRIAXYS buoy (black) and 1500 m from MORAY with ASIS buoy (gray).

3 Acoustic Measurements

The transmitted signal was a multi-frequency CW pulse of duration 3 ms for which carrier frequencies between 4 and 20 kHz (in 2 kHz increments) were superimposed and transmitted simultaneously. A particular frequency is recovered in post-processing via digital band-pass filtering (acoustic data sampled at 50 kHz). The main transmission set contained 5 other signal types spanning the frequency range 1-20 kHz, and each signal was transmitted 20 times with a signal repetition period of 8 sec. Upon completion of all transmissions, data were uploaded from the MORAY via telemetry. A second transmission set was undertaken after which the R/V *Knorr* established position at the next source station and continued the experiment. The four stations in source-receiver bearing angle were, in order of their sampling, 210°, 120°, 30° and 300°. Thus, for example, transmissions from the third station were nominally aligned with the primary direction of the surface wave field as shown in Fig. 2 (a).

The pulse length of the quasi-narrow band signals was sufficiently short to permit time resolution of individual arrivals (Fig. 3), and the emphasis of this paper is on the vertical spatial coherence of arrivals associated with the single surface bounce path. Estimates of vertical spatial coherence are made according to the approach and algorithm discussed in [5].

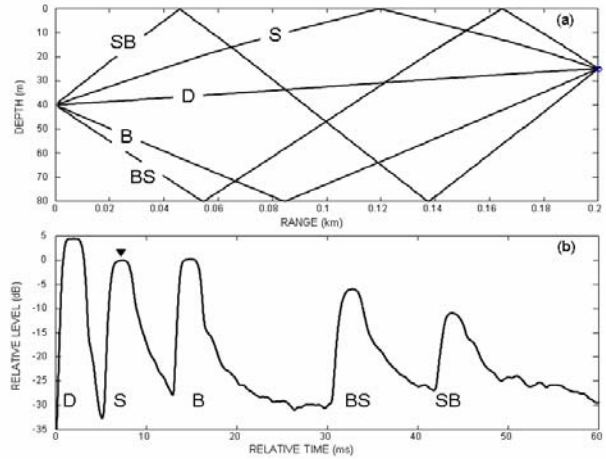

Fig. 3 (a) Ray diagram based on CTD cast made August 10th 1107 UTC (see Fig. 1), showing various arrivals for a source at depth 40 m, receiver at depth 25 m, and range 200 m. Arrivals are the direct path (D), surface path (S), bottom path (B), bottom-surface path (BS), and surface-bottom path (SB). (b) Time series of received level for 3-ms pulse of center frequency 16 kHz, based on the average of a 20-ping transmissions made on 10 Aug at 10:00 UTC. The mark above the surface path (S) denotes region of steady state return, and time window within which coherence is estimated is centered here.

Other, related investigations originating from these same experimental measurements include one on bottom interaction [3] and one on the influence of bubbles in forward scattering from the sea surface [4]. Results in [4] suggest bubbles play a minor role in forward scattering for the conditions on August 10th . (This was not the case for the much higher wind speeds, greater than 10 m/s, observed on August 15th, and results on spatial coherence for that day continue to be studied.)

4 Results

4.1 Directional Wave Effects

Estimates of vertical spatial coherence at 16 kHz plotted as function of normalized vertical receiver separation *kd* where *d* is separation and *k* is acoustic wave number are shown in Fig. 4. The data correspond to the surface path geometry of Fig. 3. The 16 kHz frequency was unique insofar as it was sampled twice, once for the aforementioned multi-frequency pulse for which 16 kHz was embedded and once for a simple, 3 ms pulse of center frequency 16 kHz. In view of the 8 sec. repetition period, these two pulses sampled an independent realization of the sea surface. With the second set of 20 transmissions there were thus four independent measurements (20 pings each) at 16 kHz, at each station. There is considerable scatter in estimates of coherence magnitude shown in Fig. 4 based on 20 pings. Of significance, however, is that there is no clear evidence that estimates are influenced by the changing source-receiver bearing angle that spans 360° between 0830 - 1500. The scatter for all four stations is about the same, and nominally consistent with the two representative error bars shown in Fig. 4. These correspond to +/- one

standard deviation of an estimate of |Γ| were it to be either 0.6 or 0.4, and based on sample average of 20. Figure 4 is evidence that directional wave properties, i.e., specifically as shown in Fig. 2 (upper), have little influence on vertical spatial coherence at a frequency of 16 kHz and above; a result consistent with [5].

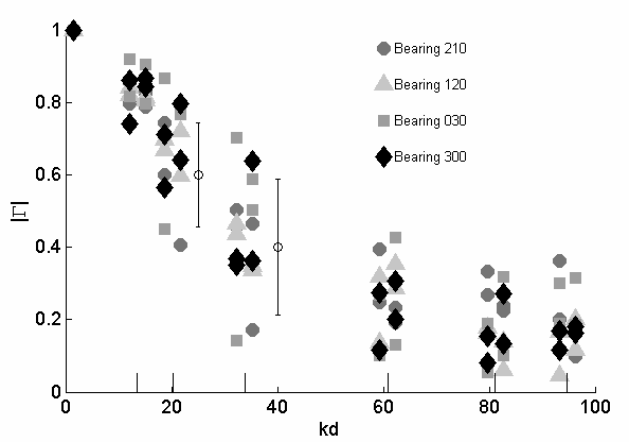

Fig.4 Absolute value of vertical spatial coherence |Γ| plotted as function of normalized receiver separation *kd* based on a center frequency of 16 kHz. Symbols correspond to the four source-receiver bearing angles identified in the legend representing four source locations. For 16 kHz, four estimates of |Γ| are available at each station. For clarity the first two estimates are plotted slightly offset the second two, and about the corresponding *kd* value (this *kd* value is identified by the vertical tick marks on the *kd* axis). Representative error bars based on 20 ping average are shown for theoretical values of |Γ| = 0.4 and 0.6.

Additional analysis suggests the same conclusion can be made of the measurements made at 14 kHz. The sea surface grazing angle θ_g is 15° and at 14 kHz the roughness parameter, $\chi = 2\,k\,H \sin\theta_g$, is greater than 5, indicating incoherent bistatic scattering from the surface at this frequency and above. In modelling (discussed below) results differ little for frequencies of 14 kHz and higher. Therefore in the following we: (1) combine results from 14 to 20 kHz to improve the sampling in *kd* space, (2) average the measurements made over the four stations between 0830-1500 to reduce statistical uncertainty, and (3) model the results based on a directionally averaged wave spectrum in view of Fig. 4. We remark here that the lower frequency data, from 12 kHz down to 1 kHz, display some effects that require a more detailed analysis of the sea surface conditions for proper interpretation, which is part of an ongoing study.

4.2 Modeling

Modeling of spatial coherence is carried out using the approach described in [5] that employs the van Cittert-Zernike theorem. Required is an estimate of the sea surface bistatic cross section computed using the small slope approximation [6], as function of position on the sea surface. For the scattering calculations we require an estimate of the directionally-averaged sea surface wave number spectrum, *F(K)*, and as the higher wave numbers in *F(K)* are not sensed by the ASIS buoy we employ a model by Plant [7], with the combined buoy plus modeled *F(K)* shown in Fig. 5.

In view of Fig. 1 we anticipate refraction effects to be influential in the modeling. Measurements similar to those discussed here were made in the East China Sea as part of ASIAEX [5]. For ASIAEX, the primary influence of refraction was to produce a small change in the phase of vertical coherence, but with a little change in coherence magnitude. This is readily understood in the context of Fig. 1, e.g., the entire sound speed versus depth variation for the late spring environment in the East China Sea lies 1520 and 1530 m/s. In contrast, the more strongly downward refracting sound speed environment in SW06 significantly changes the incident and grazing angles that determine the level of the bistatic scattering cross section, and also compresses the set of vertical arrivals at the receiver.

In terms of the bistatic scattering, the effect of refraction, as computed using the *Knorr* CTD cast in Fig. 1 is small, (Fig. 6). The downward refraction increases the maximum scattering in the vicinity of the specular point by about 1 dB, compared to iso-velocity conditions using the same *F(K),* as the over all surface appears smoother owing to decreased incident and scattered angles; specifically the parameter $\chi = k\,H\,(\sin\theta_i + \sin\theta_s)$ has been reduced.

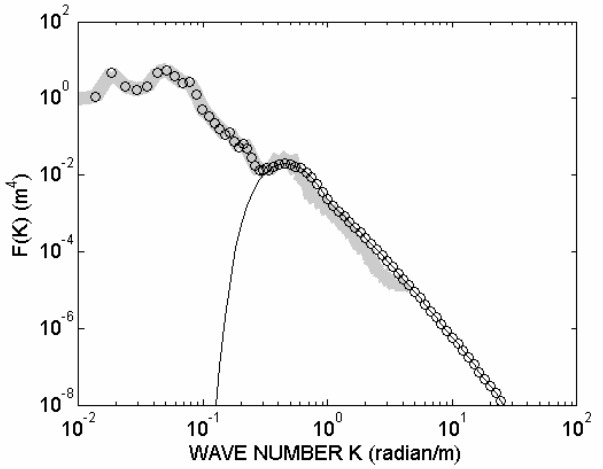

Fig.5 The directionally averaged wave number spectrum, *F(K)* used for computing the bistatic cross section of the sea surface (circles). This is based on combination the transformed directionally averaged ASIS frequency spectrum (thick, gray line) and a model for *F(K)* associated with wind waves, assuming a wind speed of 6 m/s and 30 km fetch (thin line).

The corresponding model for vertical spatial coherence displays a much more significant effect of refraction which is also consistent with the data (Fig. 7). The data in Fig. 7 represent an average over the four source stations for frequencies 14, 16, 18 and 20 kHz. Each frequency is averaged separately and results clearly scale with parameter *kd* in terms of the magnitude (circles with error bars) and real part (triangles without error bars) of vertical coherence.

The model is based on a center frequency of 20 kHz (with little change in modeling results for center frequencies down to 14 kHz). Two models are displayed in Fig. 7 one (solid decaying and oscillating lines) incorporates refraction effects and the other (dashed lines) is based on iso-velocity conditions. The real part of vertical coherence goes as

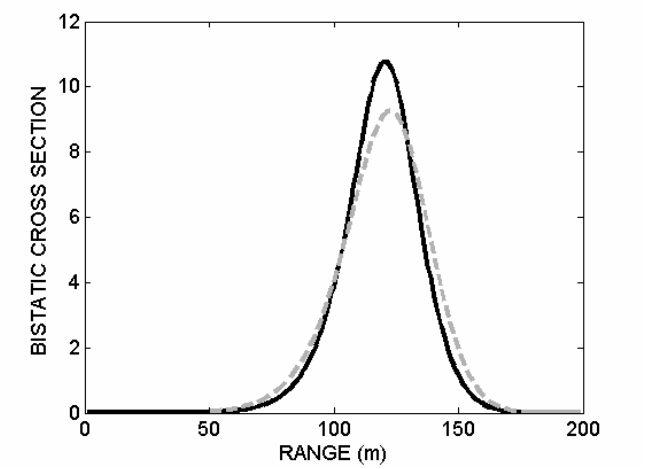

Fig.6 Bistatic cross section along the line on the sea surface connecting source with receiver (bistatic angle 0^o), incorporating refraction effects (solid line) compared with iso-velocity conditions (dashed line). Calculations are based on the *F(K)* in Fig. 5 and frequency 20 kHz. The source depth is 40 m, receiver depth 25 m, and the range is 200 m.

$\cos kd\,\bar{\theta}_V$ (to first order) where $\bar{\theta}_V$ is the mean vertical arrival angle. Given the specular grazing angle is 15^o for the sound speed profiles in Fig. 1 and array acquisition geometry of Fig. 3, this puts $\bar{\theta}_V$ at ~20^o, which describes initial oscillation at low *kd* seen in the real parts for model and data. In contrast, the model real part based on iso-velocity conditions is characterized by a $\bar{\theta}_V$ of ~18^o and is clearly out of phase with the data.

A more significant effect is the increase in coherence magnitude versus *kd* over that expected for iso-velocity conditions. For example, define *kd** as the value at which the model |Γ| equals $e^{-1/2}$; this value is 14 and 21 for the iso-velocity and refraction models, respectively. Such a large difference in *kd**, representing say the vertical coherence length of the array, is difficult to achieve based on changing rough surface conditions alone. For example, with the source-receiver geometry of Fig. 3, modelling suggests that *kd** varies by less than about 25%, over the range of input surface wave models *F(K)* that are associated with wind speeds between 4 and 11 m/s.

Let us take 1/ *kd** as an estimate of the angular variance or spread of vertical arrival angle about $\bar{\theta}_V$. The change in *kd** can be understood from Snell's Law, relating the vertical arrival angle to the launch angle at the sea surface, θ_S ,

$$\theta_V = \arccos(n\cos\theta_S) \qquad (1)$$

where n = 1485/1530 is the receiver-depth to sea surface sound speed ratio. The variance of θ_V is approximated by an expansion of Eq. (1) about $\bar{\theta}_S$, leading to

$$g = \frac{n\sin\bar{\theta}_S}{\sqrt{1-n^2\cos^2\bar{\theta}_S}} \qquad (2)$$

such that reduced angular variance (owing to refraction) is g^2 times original variance (expected in iso-velocity conditions). Using $\bar{\theta}_S$ = 15^o, g = 0.72 and *kd** should increase by a factor of 1/*g* owing to refraction, which is roughly the case.

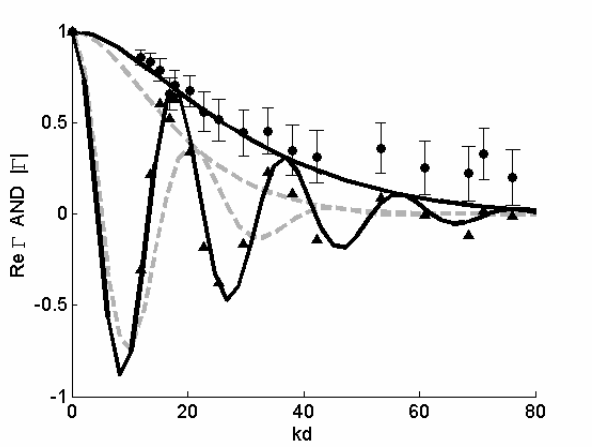

Fig.7 Absolute value of vertical spatial coherence |Γ| (solid circles with error bars) and real part Re Γ (solid triangles without error bars) plotted as function of normalized receiver separation *kd* for center frequencies 14, 16, 18 and 20 kHz. Solid lines represent a model for the absolute value and real part that incorporates refraction effects; lighter, dashed lines represent an equivalent model that assumes iso- velocity sound speed conditions.

5 Conclusion

Measurements from SW06 of the vertical coherence and related angular spreading associated with forward scattering from the sea surface have been analyzed. A systematic measurement over 4 bearing angles was carried out for 6.5 h during which the wind-wave conditions were relatively unchanging as represented by rms waveheight of 0.16 m and wind speed of 6 m/s. Primary conclusions that emerge from this analysis are:

1. For frequencies 14 kHz and above, the directional wave effects associated with the steady conditions on August 10^{th} did not have an observable influence on vertical spatial coherence. It is expected that this conclusion applies to the frequency range of O(10) kHz and above and for other wind-wave conditions.
2. Strong downward refraction compresses the vertical angular spread associated with rough sea surface scattering effects that is sensed at a receiver well below the surface. This compression can produce a change in coherence magnitude that either is on the level of, or exceeds, that associated with a large change in the sea surface wave conditions.
3. A simple model is derived to predict the compression effect based on Snell's law.

Acknowledgments

This research was supported by the Office of Naval Research. The author thanks Neil Williams and Hans Graber from University of Miami for making available the ASIS wind and wave data. Additional sound speed data were made available courtesy of the Woods Hole Oceanographic Institution, Ocean Acoustics Laboratory.

References

[1] Jee Woong Choi and Peter H. Dahl, "Measurement and simulation of the channel intensity impulse response for a site in the East China Sea," *J. Acoust. Soc. Am.* 119, 2677-2685 (2006).

[2] Dajun Tang, J. F. Moum, J. F. Lynch, P. Abbot, N. R. Chapman, P. H. Dahl, T. F. Duda, G. Gawarkiewicz, S. Glenn, J. A. Goff, H. Graber, J. Kemp, A. Maffei, J. D. Nash, and A. Newhall., "Shallow-Water '06:A Joint Acoustic Propagation/Nonlinear Internal Wave Physics Experiment," *Oceanography,* Vol. 20*,* 156-167, (2007).

[3] Jee Woong Choi, Peter H. Dahl, and John Goff, "Observations of the R-reflector and sediment interface reflection at the Shallow Water 06 Central Site," submitted to *J. Acoust. Soc. Am.* March 2008.

[4] Peter H. Dahl, Jee Woong Choi, Neil J. Williams, and Hans C. Graber , "Field measurement and modeling of attenuation from near-surface bubbles for frequencies 1-20 kHz," submitted to *J. Acoust. Soc. Am.* March 2008.

[5] Peter H. Dahl, "Forward scattering from the sea surface and the van Cittert-Zernike theorem," *J. Acoust. Soc. Am.* 115, 589-599 (2004).

[6] Peter H. Dahl, "On bistatic sea surface scattering: Field measurements and modeling," *J. Acoust. Soc. Am.* 105, 2155-2169 (1999).

[7] W. J. Plant, "A stochastic, multiscale model of microwave backscatter from the ocean," *J. Geophys. Res.* 107 10.129/2001 JC000909 (2002).